

# Method for left atrial appendage segmentation using heart CT images

Itaru Takayashiki  
Graduate School of Software and Information Science  
Iwate Prefectural University  
152-52 Sugo, Takizawashi, Iwate-ken, 020-0611 Japan  
g231r020@s.iwate-pu.ac.jp

Shoto Sekimura  
Research Institute of Systems Planning, Inc.  
18-6 Sakuragaoka-cho, Shibuya-ku, Tokyo-to, 150-0031 Japan  
sekimura@isp.co.jp

Akio Doi  
Graduate School of Software and Information Science  
Iwate Prefectural University  
152-52 Sugo, Takizawashi, Iwate-ken, 020-0611 Japan  
doia@iwate-pu.ac.jp

Maiko Hozawa  
Internal Medicine Course  
Iwate Medical University  
19-1 Uchimaru, Morioka-shi, Iwate-ken, 020-8505 Japan  
maiyan117@gmail.com

Toru Kato  
Graduate School of Software and Information Science  
Iwate Prefectural University  
152-52 Sugo, Takizawashi, Iwate-ken, 020-0611 Japan  
kato\_t@i-plants.jp

Hiroki Takahashi  
Graduate School of Software and Information Science  
Iwate Prefectural University  
152-52 Sugo, Takizawashi, Iwate-ken, 020-0611 Japan  
t-hiroki@iwate-pu.ac.jp

**Abstract—** In this study, we propose a method to automatically extract the details of the left atrial appendage region from heart CT images in order to facilitate the preoperative planning of Left Atrial Appendage Occlusion. Generally, it is difficult to automatically classify the left atrial appendage region in a heart CT image because the heart is a very complicated organ. Therefore, in addition to the segmentation method using fully convolutional neural networks, we performed an automatic extraction of only the left atrial appendage region using mini-batch and adversarial training. This method was applied to heart CT images made with a contrast medium. With this method, it becomes possible to automatically obtain information necessary for preoperative planning support of left atrial appendage closure from heart CT images.

**Keywords—** Left Atrial Appendage Region, Heart CT Image, Deep Learning, Fully Convolutional Neural Networks, Segmentation, Left Atrial Appendage Occlusion

## I. INTRODUCTION

Left atrial appendage occlusion (LAAO) has attracted attention as a method to prevent cerebral infarction due to a thrombus in the left atrial appendage. LAAO is a procedure that approaches the heart transcatheterly from the femoral vein and attaches a closure device to the left atrial appendage (Fig. 1). About 90% of cerebral infarctions that occur in patients with atrial fibrillation (AF patients) are said to be caused by thrombi formed in the left atrial appendage. LAAO is a preventive intervention for cardiogenic embolism and requires only one procedure. Therefore, it may be possible to stop administration of warfarin, with its risk of bleeding. This is reported to be cost-effective for preventing cerebral infarction for AF patients[1]. In addition, it has been reported that the risk of re-hospitalization due to thromboembolism has been reduced for 3 years after LAAO has been performed on AF patients[2]. Thus, LAAO appears to reduce cerebral infarction and overall mortality[3]. However, the left atrial appendage has a complex structure and exhibits many different forms unique to each individual. In addition, if the attachment of the left atrial appendage closure device fails, it may lead to fatal complications. Therefore, it is important to carefully grasp the left atrial appendage form to plan the surgery in advance.

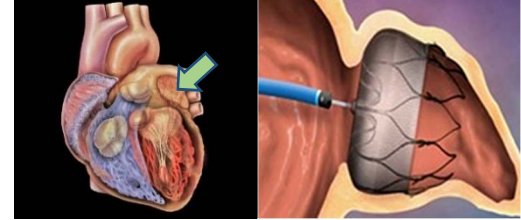


Fig. 1. Left atrial appendage area and left atrial appendage closure device. Image courtesy: [4][5].

A fully convolutional network (FCN) is a type of convolutional neural network, and it is generally used for semantic segmentation to perform pixel-by-pixel labeling or classification. However, to create labeled data, it is necessary to annotate each pixel, which makes such data difficult to obtain.

This study improved generalization performance by performing adversarial training (AT) inside a FCN. We considered the information about the left atrial appendage area extracted by this method as a way to support LAAO.

The experiment used 69 patients (69 cases) of computed tomography (CT) images obtained during administration of a contrast agent. The effectiveness of this method was verified by using these cases for training and performing tests on six cases.

## II. PREVIOUS RESEARCH

### A. Fully Convolutional Networks

FCNs, neural networks composed only of convolutions, have recently been shown to provide high accuracy in segmentation tasks. FCNs do not lose the spatial information of the object on the image by eliminating the fully connected layer[6]. They also enable image-to-image conversion and can be applied to variable image sizes. Therefore, FCNs are often used for semantic segmentation.

In addition, several networks suitable for medical image segmentation, such as V-net and U-net, are also proposed[7][8].

Phi and Christians et al. performed segmentation of the left ventricle and the right ventricle into lumen and myocardium from magnetic resonance images using a FCN[9][10]. Verification showed that segmentation using a FCN is superior to previous automatic segmentation methods. In these studies, segmentation was performed on images of the left ventricle, right atrium, and myocardium, but the left atrial appendage was not segmented.

### B. Adversarial Training

Several machine learning models, including neural networks, misclassify data when small adversarial perturbations are added that humans cannot detect. This indicates that the trained model has not been able to obtain the needed generalization performance. In other words, generalization performance can be expected to improve by performing learning on data with adversarial perturbations. Goodfellow et al. developed a regularization AT method for learning using adversarial examples (AE), in which adversarial perturbations were added to the original data[11].

Adversarial perturbations are small changes that increase the Loss of the machine learning model, mostly with respect to the input data. These adversarial perturbations can be calculated at high speed by finding the gradient for the input data using the error back-propagation method. AT can realize higher generalization performance than learning in which random noise is added to data and learning with dropout.

## III. PROPOSED METHOD

### A. Network configuration

Fig. 2 shows the structure of our FCN. The network structure consists of five layers based on the encoder-decoder type of U-Net. The image is restored by the decoder while holding the position information of the image in each layer. A  $5 \times 5$  convolution filter was used in the encoder part, and the parametric ReLU is used as the activation function after convolution. We used a  $2 \times 2$  convolution filter with Stride2 for down-sampling and a  $2 \times 2$  deconvolution filter with Stride2 for up-sampling.

It is possible to prevent gradient loss by implementing residual connections throughout the network[12]. In addition, the feature map is maintained by connecting the first and second halves of the network.

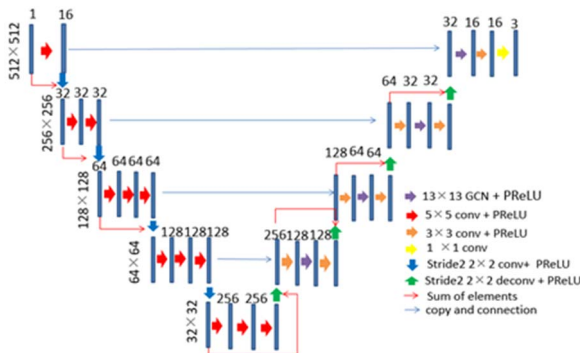


Fig. 2. FCN network structure.

### B. Loss function · Accuracy

The Loss function calculates the cross-entropy loss for each pixel of the image. The equation is

$$\text{Loss} = - \left( \sum_{h,w} \sum_{c \in C} y_n^{(h,w,c)} \log(S(x_n)^{(h,w,c)}) + \sum_{h,w} \sum_{c \in C} y_n^{(h,w,c)} \log(S(x_n+r)^{(h,w,c)}) \right), \quad (1)$$

where  $x$  is an image,  $r$  represents a hostile perturbation to deceive the virtual FCN,  $y$  is a label,  $h$  and  $w$  represent height and width,  $c$  is the number of channels,  $S$  is the FCN, and  $S(x)$  is a segmentation result.

In this research, accuracy is calculated by the intersection over union method as follows:

$$\text{Accuracy} = \frac{T \cap G}{T \cup G}, \quad (2)$$

where  $T$  represents the segmented data and  $G$  represents labeled data. Equation (2) calculates how much of the combined area of  $T$  and  $G$  is included in the target area.

### C. Data set creation method

In this study, we used 69 cases of multi-slice CT images of a heart, which was imaged during administration of a contrast medium. The imaging conditions are standardized at the isovolumetric relaxation phase (timing at 50% where the interval between R waves is 100%) before the ventricular diastole. In the isovolumic relaxation phase, the ventricular volume does not change until the ventricles contract. Labeling data were created for all 69 cases of heart CT images.

3D visualization volume extractor software was used to create labeled data. The left atrial appendage region was extracted from the original image data displaying the entire heart by repeating the clipping operation about 15 to 20 times (Fig. 3). The extracted left atrial appendage region was binarized with 0 representing background and 1 representing the left atrial appendage region. Fig. 4 shows the created labeled data.

The creation of labeled data requires appropriate knowledge of and experience in image interpretation. In addition, it is necessary to annotate each pixel, and this work must be performed on all slices. Therefore, the burden of labeled data creation is large. In the case of the labeled data used in this study, the preparation time per case was about 30 min.

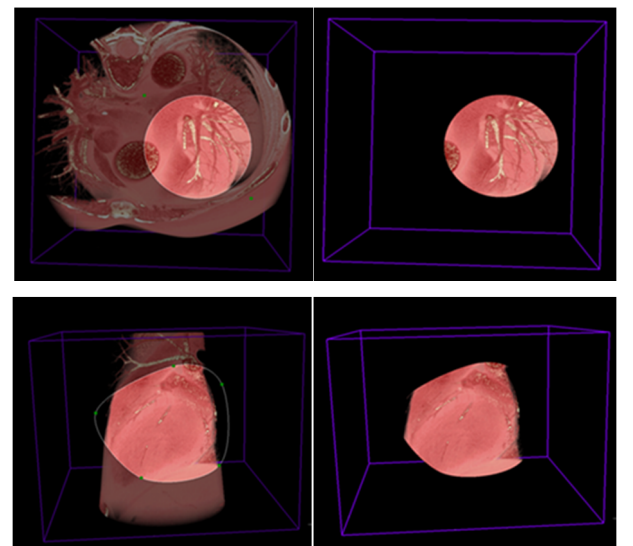


Fig. 3. Clipping process.

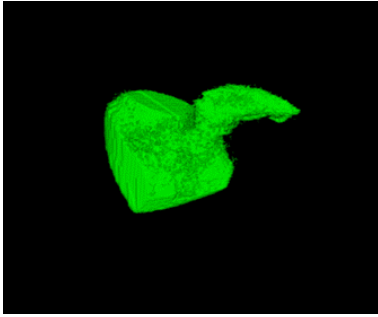


Fig. 4. Labeled data for left atrial appendage area.

#### D. Mini-batch learning method

In this study, learning was performed on sliced image units. Therefore, convergence takes a long time when learning is performed by reading slices one by one. In addition, accuracy was not stable because some slice images were only background. As a result, we could process multiple image slices at one time by employing mini-batches during learning. This made it possible to stabilize Accuracy and Loss. In this study, the mini-batch size was six.

#### E. How to create Adversarial Example

This study improved the generalization performance of the FCN by performing AT. As mentioned above, AT learns AE and improves the generalization ability. Specifically, Miyato's method[13] was used to create AE with the following equation:

$$AE = x + \epsilon \frac{g}{\|g\|}. \quad (3)$$

AE are created by adding the original data "x" and the adversarial perturbation. In this way, the adversarial perturbation is calculated so that the Loss of the machine learning model is the largest and can be approximately calculated by the error back-propagation method. This method is commonly used in the training of neural networks and can also calculate the gradient for the weight parameter efficiently. If the original datum x is regarded as a weight parameter, application of the error back-propagation method can calculate the gradient g for the original datum x. By using gradient g, it can be understood what kind of change was made in the original datum x to increase the Loss value. Adversarial perturbations can be calculated by dividing gradient g of the original data by the Euclidean norm of gradient g and multiplying it by a parameter  $\epsilon$  that controls the magnitude of the change.

In this study,  $5e+4$  was used for  $\epsilon$  when finding the AE for the original image. In addition, when creating AE for labeled data and the segmentation image, 2.0 was used for  $\epsilon$ .

## IV. EVALUATION

#### A. Verification approach

For verification, we used 69 cases of voxel data of multi-slice CT of the heart imaged with a contrast agent. Of these, 63 cases were used for training and 6 cases were used for testing. The size of each dataset was  $512 \times 512$  in x-y, and the number of slice images differed depending on each dataset. The effectiveness of this method was verified by training and testing these data with the FCN and a mini-batch size of six.

The verification environment was as shown in TABLE I. TABLE II shows the training period and test time per case.

TABLE I. VERIFICATION ENVIRONMENT

CPU	Intel® Core™ i7-8700k CPU @ 3.70 GHz
GPU	GeForce GTX 1080Ti $\times$ 2
RAM	64 GB (16 GB $\times$ 4)
OS	Ubuntu 16.04
Execution environment	Python 3.5, TensorFlow-gpu 1.4, Cuda 8.0

TABLE II. TRAINING PERIOD AND TEST TIME

Training period	Number of trials	Test time (per case)
11 days	5,350	$\sim$ 3 min

#### B. Training and test results

Figs. 6 and 7 show graphs of changes in accuracy and Loss during training. It can be seen that the average accuracy was 0.884 (88.4%), a high value. The accuracy is higher as it approaches 1. The Loss value represents the difference between the result and the correct answer, and it is considered to be better as it approaches 0. The Loss graph shows that the Loss decreased as the number of learning iterations (mini-batches) increased. However, sometimes the value repeatedly rose and fell. This is considered to be due to the differences in the accuracy between each slice image input by mini-batch. Enlargement of the mini-batch size may reduce this effect.

TABLE III shows the results of tests conducted on six cases. The average testing accuracy was 0.623 (62.3%), with the first case showing the highest value (0.684, or 68.4%), and the third case showing the lowest value (0.518, or 51.8%). It seems to be possible to improve the accuracy by increasing the number of training cases and using a higher-performance workstation. However, comparison of the first case with the highest accuracy and the third case with the lowest shows that the visual difference is small. This indicates that the left atrial appendage region can be correctly segmented (Fig. 7).

From these results, although learning took a long time, it is considered to be sufficiently useful in consideration of the effort and time required to create learning data from medical images.

#### C. Support for left atrial appendage occlusion planning

Transesophageal echocardiography is often used to evaluate cardiac valvular disease and cardiac structural disease. In this method, an ultrasound endoscope about 1 cm in diameter is passed from the mouth to the esophagus. The doctor manually adjusts the depth of the probe and its fan-like ultrasound irradiation angle while referring to only the echo image. Therefore, it takes time and is uncomfortable

for the patient. Furthermore, it is difficult to grasp the 3D position of the heart only with echo images. Therefore, we used our CNF to construct a transesophageal echocardiography support system using heart CT images for preoperative planning for LAAO. We believe that this will greatly shorten the procedure time and reduce the burden on patients.

The left atrial appendage region information automatically extracted by FCN highlights the left atrial appendage region and assists in manual estimation of the camera that displays the left atrial appendage region image clearly. Fig. 8 shows the user interface of this system, which provides buttons and dials reflecting the actual path of the echocardiography device. Fig. 9 is an example of a cross-sectional view along the centerline of the transesophageal echocardiograph. Fig. 10 shows an example of the screen display when the distance and area of the left atrial appendage area are measured. In this figure, the red text is the distance and the yellow text is the area.

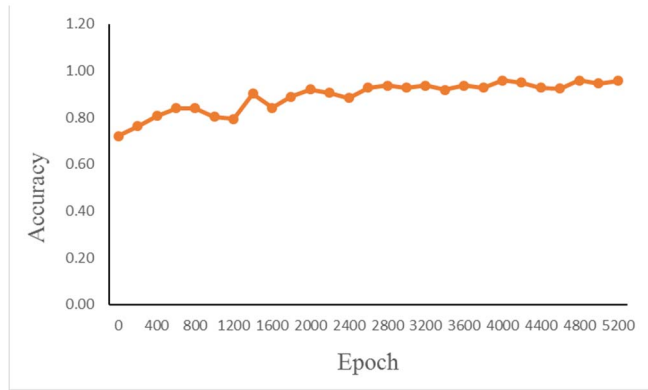


Fig. 5. Evolution of accuracy.

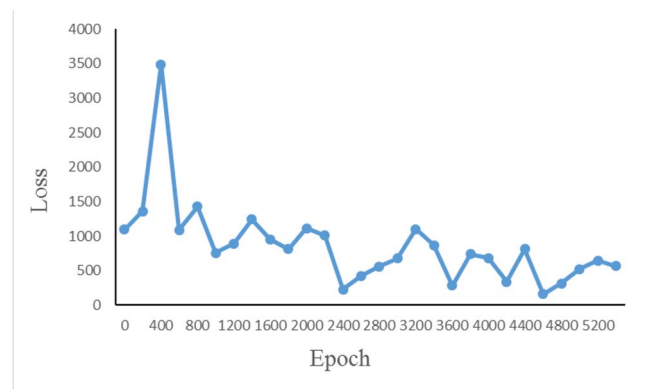


Fig. 6. Evolution of Loss.

TABLE III. TEST RESULTS

Measure	1	2	3	4	5	6	Average
Accuracy	0.684	0.629	0.518	0.677	0.603	0.628	0.623
Loss	4,999	5,025	9,837	7,953	3,592	3,304	5,784.9

Test time	2 min 50 s	3 min	2 min 40 s	2 min 35 s	3 min 10 s	2 min 50 s	2 min 51 s

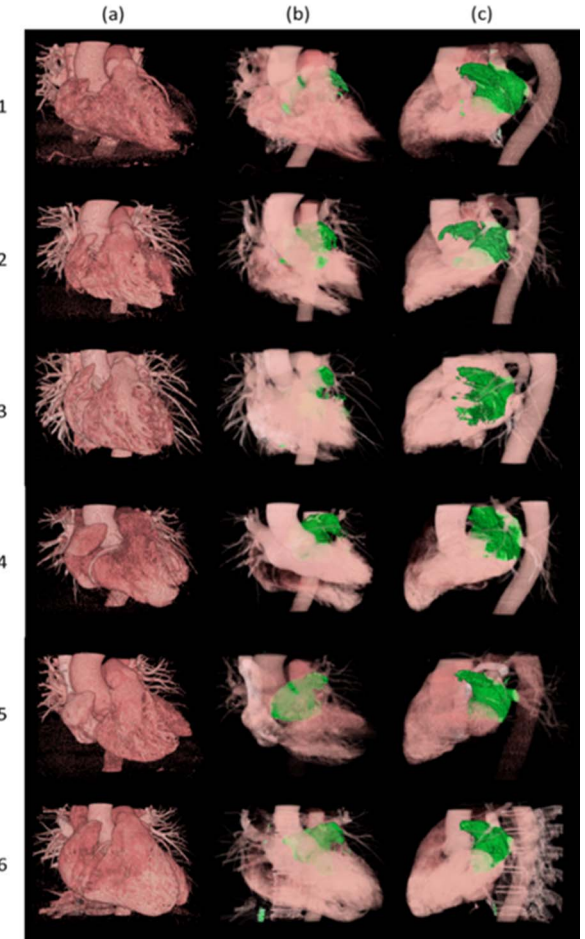


Fig. 7. Six segmented views of left atrial appendage area. (a) Front view of original image, (b) Front view of evaluation result of left atrial appendage, (c) Side view.

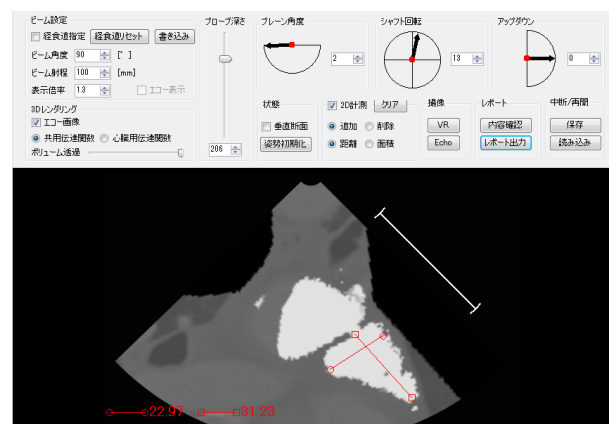


Fig. 8. Transesophageal imaging diagnosis using heart CT images.

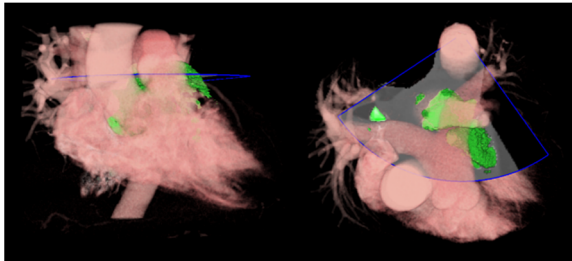


Fig. 9. Cross-sectional view along the transesophageal echocardiograph.

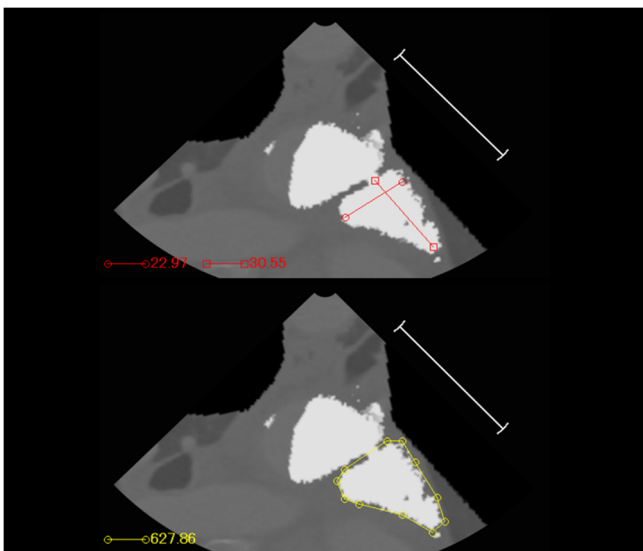


Fig. 10. This is a screen that measures distance and area.

## V. CONCLUSION

In this paper, we proposed a segmentation method to extract left atrial appendage region efficiently from cardiac CT images produced with a contrast agent. The number of epochs until convergence was large because learning was performed on small batches of image slices extracted from 3D images. However, we think that improvement is possible by enlarging the mini-batch size. In addition, it was possible to improve the generalization performance of FCN by using AT.

The FCN model in this method can extract the left atrial appendage region from a heart CT image with high accuracy, and by using its position information, it can be applied to LAAO.

As future deployment, we will consider the use of a deep convolutional generative adversarial network (DCGAN)[14]. It is difficult to obtain labeled data for medical images. Therefore, the lack of learning data imposes a great restriction on the network performance. Therefore, the number of training images can be increased by applying DCGAN and performing semi-supervised learning by FCN. This is considered to enable high-precision learning with a small amount of labeled data. We also will examine the results of increasing the number of cases and mini-batch size.

## ACKNOWLEDGMENT

For this study, we received research grants from the “Research and development support project of cardiac quantification software to support the 2017 cardiac catheter surgery” of the Public Interest Incorporated Foundation JKA. We thank the foundation very much.

## REFERENCES

- [1] Reddy VY, et al., “Time to cost-effectiveness following stroke reduction strategies in AF: warfarin versus NOACs versus LAA Closure,” *J Am Coll Cardiol*. 2015;66:2728-39, 2015.
- [2] Yao X, et al., “Association of Surgical Left Atrial Appendage Occlusion With Subsequent Stroke and Mortality Among Patients Undergoing Heart Surgery,” *J American Medical Association (JAMA)*. 2018; 319(20):2116-2126, 2018.
- [3] Alli O, et al., “Quality of life assessment in the randomized PROTECT AF trial of patients at risk for stroke with non-valvular atrial fibrillation,” *J Am Coll Cardiol*, 2013; 61(17):1790-8. doi:10.1016/j.jacc.2013.01.061.
- [4] WIKIMEDIA COMMONS. Category:Medical illustrations by Patrick Lynch, Retrieved June 10, 2019, from [https://commons.wikimedia.org/wiki/Category:Medical\\_illustrations\\_by\\_Patrick\\_Lynch#/media/File:Heart\\_anterior\\_normal\\_anatomy.jpg](https://commons.wikimedia.org/wiki/Category:Medical_illustrations_by_Patrick_Lynch#/media/File:Heart_anterior_normal_anatomy.jpg)
- [5] YOONHO KIM. Survey Research: Catheter-based Treatments, Retrieved June 10, 2019, from <http://www.yoonho-kim.com/survey-reserch.html>
- [6] Jonathan Long, Evan Shelhamer, and Trevor Darrell, “Fully Convolutional Networks for Semantic Segmentation,” *The IEEE Conference on Computer Vision and Pattern Recognition (CVPR)* June 2015, pp. 3431-3440.
- [7] Olaf Ronneberger, Philipp Fischer, and Thomas Brox, “U-Net: Convolutional Networks for Biomedical Image Segmentation,” *arXiv:1505.04597v1 [cs.CV]* 18 May 2015.
- [8] Fausto Milletari, Nassir Navab, and Seyed-Ahmad Ahmadi, “V-Net: Fully Convolutional Neural Networks for Volumetric Medical Image Segmentation,” *arXiv:1606.04797v1 [cs.CV]* 15 Jun 2016.
- [9] Phi Vu Tran, “A Fully Convolutional Neural Network for Heart Segmentation in Short-Axis MRI,” *arXiv:1604.00494v3 [cs.CV]* 27 Apr 2017.
- [10] Christian F. Baumgartner, Lisa M. Koch, Marc Pollefeys, and Ender Konukoglu, “An Exploration of 2D and 3D Deep Learning Techniques for Heart MR Image Segmentation,” *arXiv:1709.04496v1 [cs.CV]* 13 Sep 2017.
- [11] Ian J. Goodfellow, Jonathon Shlens, and Christian Szegedy, “Explaining and Harnessing Adversarial Examples,” *arXiv:1412.6572v3 [stat.ML]*, 2015.
- [12] Kaiming He, Xiangyu Zhang, Shaoqing Ren, and Jian Sun, “Deep Residual Learning for Image Recognition,” *arXiv:1512.03385 [cs.CV]* 10 Dec 2015.
- [13] Takeru Miyato, Shin-ichi Maeda, Masanori Koyama, and Shin Ishii, “Virtual Adversarial Training: a Regularization Method for Supervised and Semi-supervised Learning,” *arXiv:1704.03976v1 [stat.ML]* 13 Apr 2017.
- [14] Alec Radford, Luke Metz, and Soumith Chintala, “Unsupervised Representation Learning with Deep Convolutional Generative Adversarial Networks,” *arXiv:1511.06434v1[cs.LG]* 19 Nov 2015.